



INTERNATIONAL ATOMIC ENERGY AGENCY  
UNITED NATIONS EDUCATIONAL, SCIENTIFIC AND CULTURAL ORGANIZATION  
**INTERNATIONAL CENTRE FOR THEORETICAL PHYSICS**  
I.C.T.P., P.O. BOX 586, 34100 TRIESTE, ITALY, CABLE: CENTRATOM TRIESTE



H4.SMR/773-15

**College on Medical Physics:  
Radiation Protection and Imaging Techniques**

5 - 23 September 1994

*Reconstruction from Projections Basics*

E.M. Staderini

Università degli Studi di Roma  
"La Sapienza"  
Centro per Ingegneria Biomedica  
Roma

# **RECONSTRUCTION FROM PROJECTIONS BASICS**

**Dr. Enrico M. Staderini**

*Centro Interdipartimentale di Ricerca per l'Analisi dei  
Modelli e dell'Informazione nei Sistemi Biomedici*

*University of Rome "La Sapienza"*

*Corso Vittorio Emanuele II, 244 00186 ROME Italy*

**College on Medical Physics:**

**Radiation Protection and Imaging Techniques**

**IAEA UNESCO International Centre for Theoretical Physics**

**Trieste, Italy, 5-23 September 1994**

Dear colleagues,

this lecture will be mainly focused on the mathematics underlying the image reconstruction from projections and the basic fundamentals of computed tomography (CT) and nuclear magnetic resonance (MR) will be covered.

In the first part of the seminar the physics and technology of computed tomography applications will be reviewed along with the basics of x-ray interaction with matter.

In the second part of the lesson the reconstruction methods will be presented starting with the well known and widely used transform methods (e.g. convolution backprojection) and ending with the iterative (algebraic) methods.

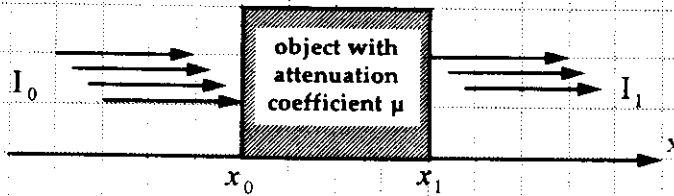
Finally, and in the exercise lessons, we will be concerned with errors in reconstructed images arising from technical, physical, mathematical and numerical analysis problems as the images we reconstruct are nothing but an approximation of what we shall never reach: reality.

So I would like to give you my greetings using a sentence a Byte magazine editor wrote a few years ago:

"Welcome in the world of numerical analysis where nothing equals itself".

## Ray interaction with matter

$$\frac{dI}{dx} = -\mu \cdot I \quad I_1 = I_0 \cdot e^{-\mu \cdot (x_1 - x_0)}$$



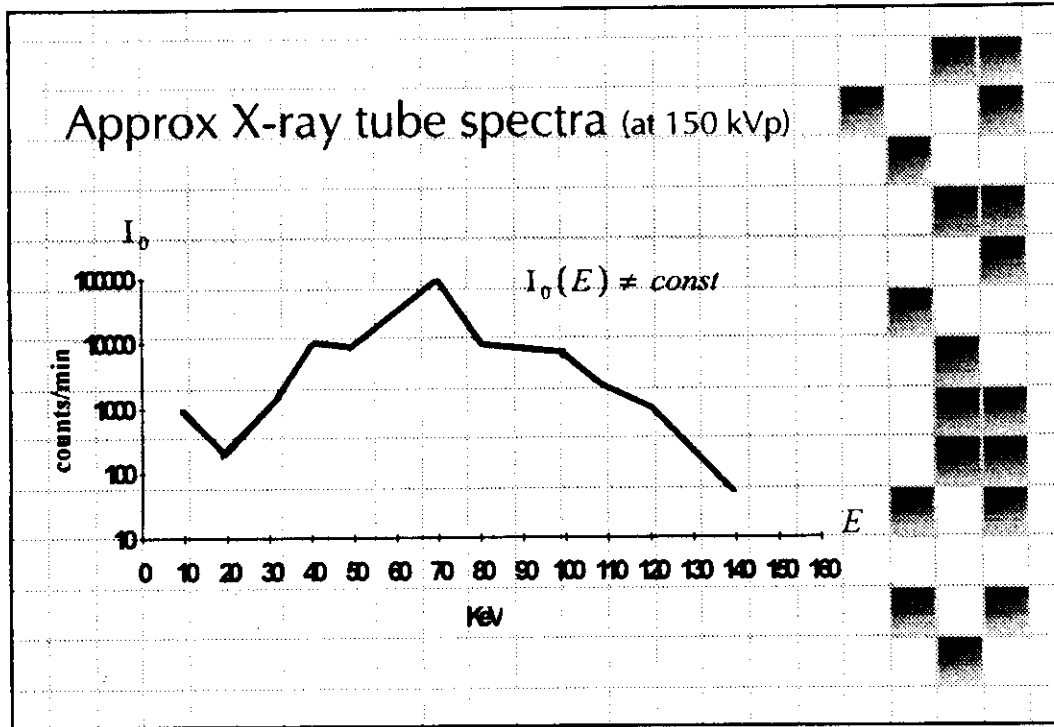
$$\mu = f(E, Z, \rho, \text{polarization}, x, y, z)$$

### RAY INTERACTION WITH MATTER

The figure above shows the effect of linear attenuation of a beam of intensity  $I_0$  when passing through an absorbing medium. The linear attenuation coefficient  $\mu$  is a function of the energy of the photons and of the atomic number and density of the matter. If the object is not homogeneous (as in real practice), then  $\mu$  is also a function of the spatial coordinates. Dicroic effects (ray polarization dependance) are present too, although of little practical importance in X-Ray computed tomography.

As the use of monochromatic X-Ray sources is impractical in biomedical computed tomography (due to low emission and consequently high acquisition times) one is forced to employ conventional X-Ray tubes whose intense emission is all but monochromatic (see following figure on next page). So only the mean of  $\mu$  over present energies can be measured:

$$I = \int_{E_1}^{E_2} I_0(E) \cdot e^{-\bar{\mu} \cdot \Delta x} \cdot dE \quad [1].$$



### RAY INTERACTION WITH MATTER

In different photon-matter interactions we have different attenuation coefficients.

For energies from 10 keV to 2 MeV we may have:

a) photoelectric interaction:

$$\mu = K \cdot \left( \frac{1}{E^{3.5}} \right) \cdot Z^4 \quad [2]$$

b) Compton interaction:

$$\mu = K \cdot Z \cdot f(E) \quad [3]$$

c) pair production: (when  $E > 1.02 \text{ MeV}$ )

$$\mu = K_1 \cdot Z^2 \cdot \ln \frac{2 \cdot E}{M_0 \cdot c^2} - K_2 \quad [4]$$

In practice a sort of "optimal" photon energy is chosen to get advantage of different attenuation coefficients trying to enhance image contrast and statistical quality.



## Physics and technology of CT applications

The physics and technology of computed tomography (CT) applications are summarized in the following slides (modified from [1]).

The emanations (i.e. the sources of energy) used to test the object are listed in the slides along with the measured physical quantities and the type of transducers most usefully employed.

This is to remind both the large number of technological possibilities available nowadays to perform a computed tomography, and the vast application field for the various methods of image reconstruction from projections.

Most used emanations are X-rays, acoustic waves, magnetic and radio-frequency electro-magnetic fields, which have permitted the research and development of practical systems for CT, echography and NMR (nuclear magnetic resonance) tomography.

## Physics and technology of CT applications

- \* Emanations used
  - \* **X-ray sources**
- \* Densities measured
  - \* **attenuation coefficients**
- \* Transducers employed
  - \* **X-ray sources**
  - \* **scintillation detectors**
- \* Applications
  - \* **Diagnostic radiology**
  - \* **Non Destructive Testing**

## Physics and technology of CT applications

- \* Emanations used
  - \*  **$\gamma$ -rays**
- \* Densities measured
  - \* **concentration of radio-labeled substance**
- \* Transducers employed
  - \* **scintillation counters**
- \* Applications
  - \* **Diagnostic radiology**
  - \* **Nuclear medicine**

## Physics and technology of CT applications

- \* Emanations used
  - \* **Compton scattered X-rays**
  - \*  **$\gamma$ -rays**
- \* Densities measured
  - \* electron density
  - \* distribution of atomic number
- \* Transducers employed
  - \* X-ray sources
  - \* scintillation counters
- \* Applications
  - \* Diagnostic radiology
  - \* Non Destructive Testing
  - \* X-ray crystallography

## Physics and technology of CT applications

- \* Emanations used
  - \* **Heavy particles**
- \* Densities measured
  - \* scattering/absorption cross-section
- \* Transducers employed
  - \* linear accelerators
  - \* stacked detectors
- \* Applications
  - \* Diagnostic radiology
  - \* Non Destructive Testing

## Physics and technology of CT applications

- \* Emanations used
  - \* **Electron beams**
- \* Densities measured
  - \* Schrodinger potential distribution
- \* Transducers employed
  - \* electron guns
  - \* film
  - \* photomultiplier/TV
- \* Applications
  - \* Microscopy

## Physics and technology of CT applications

- \* Emanations used
  - \* **Acoustic waves**
- \* Densities measured
  - \* attenuation
  - \* refractive index
  - \* acoustic impedance
- \* Transducers employed
  - \* electromechanical devices
- \* Applications
  - \* Diagnostic radiology
  - \* Non Destructive Testing
  - \* Geological prospecting



## Physics and technology of CT applications

- \* Emanations used
  - \* **Low frequency electric currents**
- \* Densities measured
  - \* electrical conductivity distribution
- \* Transducers employed
  - \* electrodes
- \* Applications
  - \* Diagnostic radiology
  - \* Non Destructive Testing
  - \* Imaging of blood vessels

## Physics and technology of CT applications

- \* Emanations used
  - \* **Magnetic fields**
- \* Densities measured
  - \* distribution of nuclear spins
  - \* blood flow
- \* Transducers employed
  - \* magnets
  - \* RF coils
  - \* magnetometers
- \* Applications
  - \* Nuclear magnetic resonance
  - \* Magneto Hydro Dynamic imaging

## Physics and technology of CT applications

- \* Emanations used
  - \* **Radio-frequency fields**
- \* Densities measured
  - \* electron spins permittivity and conductivity distribution
- \* Transducers employed
  - \* capacitors
  - \* coils
  - \* antennas
  - \* horns
- \* Applications
  - \* Nuclear magnetic resonance
  - \* Mapping

## Physics and technology of CT applications

- \* Emanations used
  - \* **Spatially incoherent electromagnetic radiations**
- \* Densities measured
  - \* volume temperature distributions
  - \* celestial brightness distribution
- \* Transducers employed
  - \* antennas
  - \* horns
  - \* telescopes
- \* Applications
  - \* Mapping temperature distribution
  - \* Astronomical imaging



## Techniques for CT applications

As far as the control extension on the sources employed is concerned, three main tomography techniques may be defined.

When the sources are emitting from inside the body, the experimenter can do nothing over them but remotely sense their emanations coming from the body. This operation is called remote sensing computed tomography.

Another aspect of computed tomography concerns the use of sources applied externally of the body and measuring the emanations passed through the object. This is the remote probing computed tomography.

In combined probing-sensing computed tomography, we deal with emanations generated from sources placed inside the body after a sort of stimulation or excitation derived from external emanations.

## Techniques of CT applications

### REMOTE-SENSING CT

- \* Single Photon Emission Computed Tomography (SPECT)
- \* Positron Emission Tomography (PET)
- \* Super Synthesis
  - Earth rotation synthesis telescope

## Techniques of CT applications

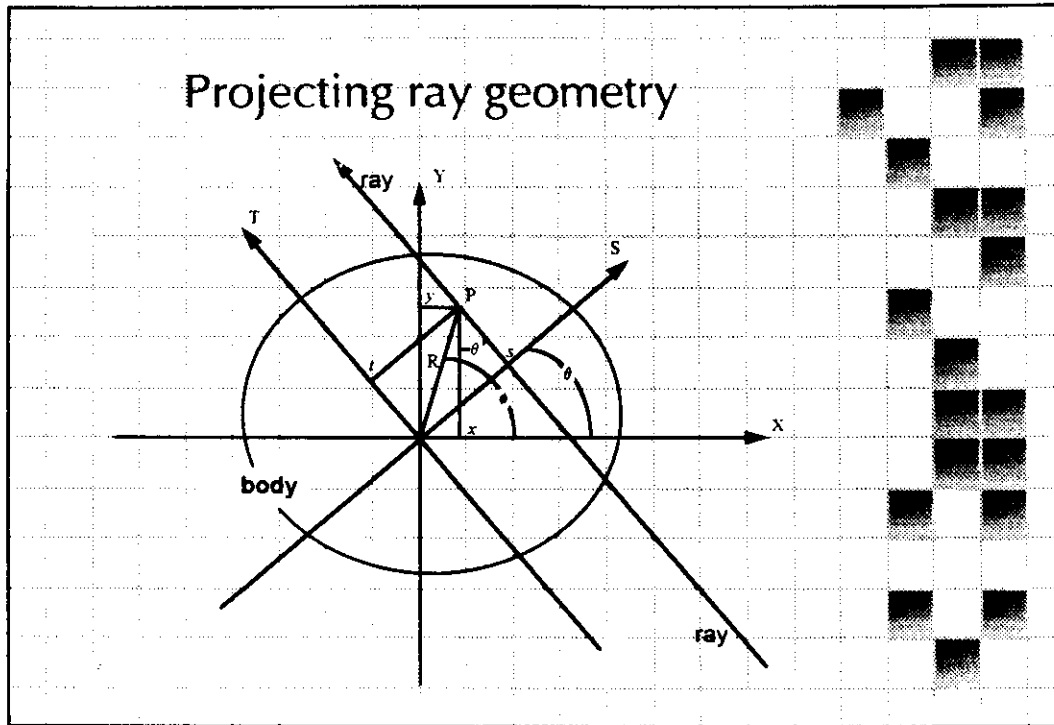
### REMOTE-PROBING CT

- \* Transmitted X-rays (Computed Tomography)
- \* Transmitted Heavy Particles
- \* Reflected/Transmitted Ultrasound
- \* Reflected Radiowaves (RADAR)
- \* Electrical Impedance
- \* Electron Microscopy

## Techniques of CT applications

### REMOTE-PROBING-SENSING CT

- \* Nuclear Magnetic Resonance (NMR)
- \* Corrected/Uncorrected Compton Scatter
- \* Magneto-Hydro-Dynamic



### GEOMETRICAL ASPECTS OF THE RECONSTRUCTION

First of all let us consider the projection ray geometry. In the figure above a circular body, whose attenuation coefficient on section  $z$  has to be measured, is passed through by a ray having an angle  $\theta$  and a displacement  $s$  with respect to the center of the body coordinates.

In the body  $z$  plane the coordinates  $(x, y)$  of the point  $P$  may be expressed in terms of  $s$  and  $\theta$  as:

$$x = R \cdot \cos(\phi) = s \cdot \cos(\theta) - t \cdot \sin(\theta) \quad [5]$$

$$y = R \cdot \sin(\phi) = s \cdot \sin(\theta) + t \cdot \cos(\theta) \quad [6]$$

The inverse relation also holds:

$$s = x \cdot \cos(\theta) + y \cdot \sin(\theta) \quad [7]$$

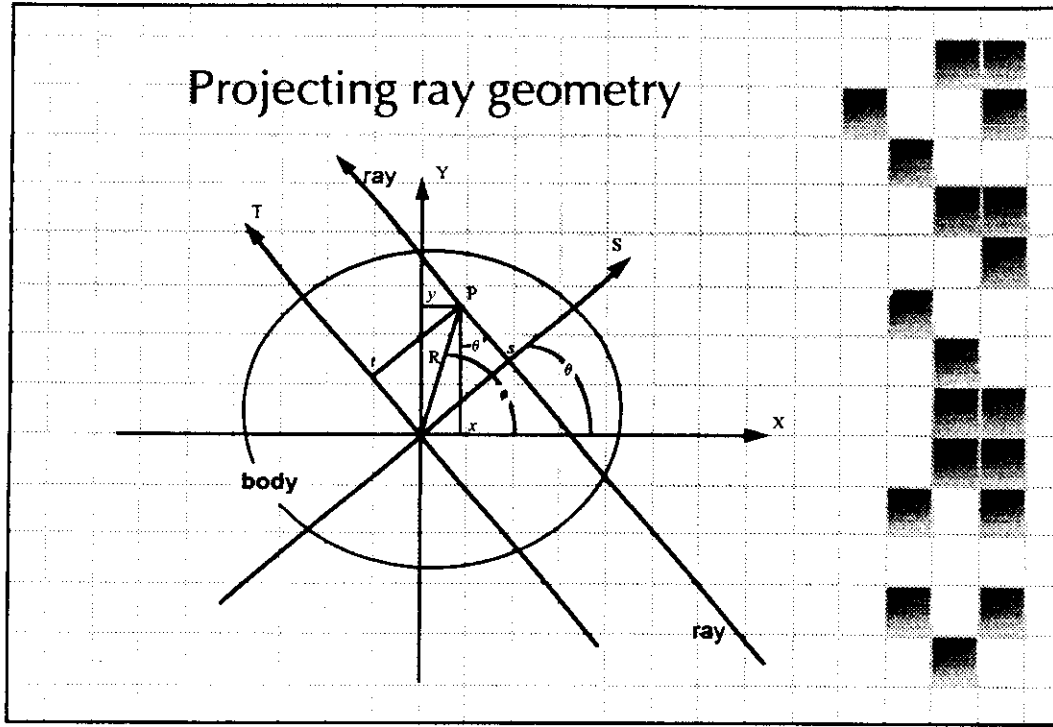
$$t = y \cdot \cos(\theta) - x \cdot \sin(\theta) \quad [8]$$

The problem of tomographic reconstruction from projections is simply to find in the section plane  $X, Y$  at  $z$ , the function [9] which provides the distribution of the physical variable  $V$  to be estimated:

$$V = f(x, y) \quad [9]$$

given the set of projections for each angle  $\theta$  and displacement  $s$  :

$$p(s, \theta) = \int_{-T}^T f(s \cdot \cos(\theta) - t \cdot \sin(\theta), s \cdot \sin(\theta) + t \cdot \cos(\theta)) \cdot dt \quad [10]$$



Where:

$$T(s) = (1 - s^2)^{\frac{1}{2}} \quad |s| \leq 1 \quad [11]$$

and:

$$p(s, \theta) = 0 \quad |s| > 1 \quad [12]$$

Please note that we are not in presence of a polar system of coordinates as:

$$p(0, \theta_1) \neq p(0, \theta_2) \quad [13]$$

Note also the periodism:

$$p(s, \theta) = p(-s, \theta + \pi) \quad [14]$$

Being the linear attenuation coefficient the physical variable whose distribution in the plane  $X, Y$  is to be estimated, we can write from [9]:

$$\mu_{x,y} = f(x, y) \quad [15]$$

So the intensity of the ray passing at displacement  $s$  and angle  $\theta$  is:

$$I(s, \theta) = I_0 \cdot e^{-\int_{s, \theta} \mu_{x,y}(x, y) dt} \quad [16]$$

where  $I_0$  is the initial intensity of the ray emitted from the X-ray source.

And for the projection we practically have:

$$p(s, \theta) = \int_{s, \theta} \mu_{x,y}(x, y) dt = \ln \left( \frac{I_0}{I(s, \theta)} \right) \quad [17].$$

## TRANSFORM METHODS

In the transform methods the problem of reconstruction from projections is faced by formulating a mathematical model in which known and unknown quantities are functions, the arguments of which come from a continuum of real numbers. Then solving for the unknown function with an inversion formula and adapting this formula for discrete or noisy data [2].

The generalized projection theorem is the basis for understanding the two most important transform methods of reconstruction.

For any given angle  $\theta$  the following relation holds:

$$\int_{-1}^1 p(s, \theta) \cdot W(s) \cdot ds = \iint_{\Omega} f(x, y) \cdot W(x \cdot \cos(\theta) + y \cdot \sin(\theta)) \cdot dx \cdot dy \quad [18]$$

The proof is simply obtained by substituting the left side using [10] and then converting from rotated coordinates using [7] and [8].

An obvious application of this theorem is obtained by using:

$$W(s) = e^{-j \cdot 2 \cdot \pi \cdot R \cdot s} \quad [19]$$

In this case it will follow that the 1-D Fourier transform of the projection at angle  $\theta$  is equal to the central slice, at the same angle, of the 2-D Fourier transform of the resulting image. This theorem is often known as the **projection-slice theorem** or the **central-section theorem** and it allows for the practical reconstruction algorithm using the Fourier transform.

Now let us consider the last theorem which can be stated in the following way:

$$\hat{p}(R, \theta) = \hat{f}(R \cdot \cos(\theta), R \cdot \sin(\theta)) \quad [20]$$

It is the central-section theorem where  $\hat{p}(R, \theta)$  is the 1-D Fourier transform of the projection  $p(s, \theta)$  with respect to the first variable.

Taking the inverse Fourier transform of [20] we obtain:

$$f(x, y) = \int_0^\pi \int_{-\infty}^\infty \hat{p}(R, \theta) \cdot e^{j \cdot 2 \cdot \pi \cdot R \cdot (x \cdot \cos(\theta) + y \cdot \sin(\theta))} \cdot |R| \cdot dR \cdot d\theta \quad [21]$$

As the following identity holds:

$$\hat{p}(R, \theta) = \int_{-1}^1 p(s, \theta) \cdot e^{-j \cdot 2 \cdot \pi \cdot R \cdot s} \cdot ds \quad [22]$$

for the projection angle  $\theta$ , and considering that we have to deal with sampled data (i.e. we have to use a window function  $W(R)$  in order to obtain a band limited reconstructed image  $f_B(x, y)$  we have:

$$f_B(x, y) = \int_0^\pi \int_{-\Delta S/2}^{\Delta S/2} \hat{p}(R, \theta) \cdot W(R) \cdot e^{j \cdot 2 \cdot \pi \cdot R \cdot (x \cdot \cos(\theta) + y \cdot \sin(\theta))} \cdot |R| \cdot dR \cdot d\theta \quad [23]$$

Using [22] we obtain:

$$f_B(x, y) = \int_0^\pi \int_{-\Delta S/2}^{\Delta S/2} \int_{-1}^1 p(s, \theta) \cdot e^{-j \cdot 2 \cdot \pi \cdot R \cdot s} \cdot W(R) \cdot e^{j \cdot 2 \cdot \pi \cdot R \cdot (x \cdot \cos(\theta) + y \cdot \sin(\theta))} \cdot |R| \cdot ds \cdot dR \cdot d\theta \quad [24]$$



Now considering the following functions:

$$q(s) = \int_{-\Delta s/2}^{\Delta s/2} |R| \cdot W(R) \cdot e^{j2\pi R s} \cdot dR \quad [25]$$

$$\hat{q}(R) = |R| \cdot W(R) \quad [26]$$

we have:

$$f_B(x, y) = \int_0^\pi \int_{-1}^1 p(s, \theta) \cdot q(x \cdot \cos(\theta) + y \cdot \sin(\theta) - s) \cdot ds \cdot d\theta \quad [27]$$

after having interchanged the order of integration over s and R.

Note now that the problem of reconstructing the function  $f_B(x, y)$  may be split into two parts.

First we can integrate over s and then integrate over  $\theta$ .

We obtain:

$$\tilde{p}(s', \theta) = \int_{-1}^1 p(s, \theta) \cdot q(s' - s) \cdot ds \quad [28]$$

which is mathematically a convolution of  $p(s, \theta)$  using the function q as the convolution kernel.

Then we have:

$$f_B(x, y) = \int_0^\pi \tilde{p}(x \cdot \cos(\theta) + y \cdot \sin(\theta), \theta) \cdot d\theta \quad [29]$$

in which the parameters of the function p are nothing but the parameters of a ray passing through the point (x,y) at angle  $\theta$ .

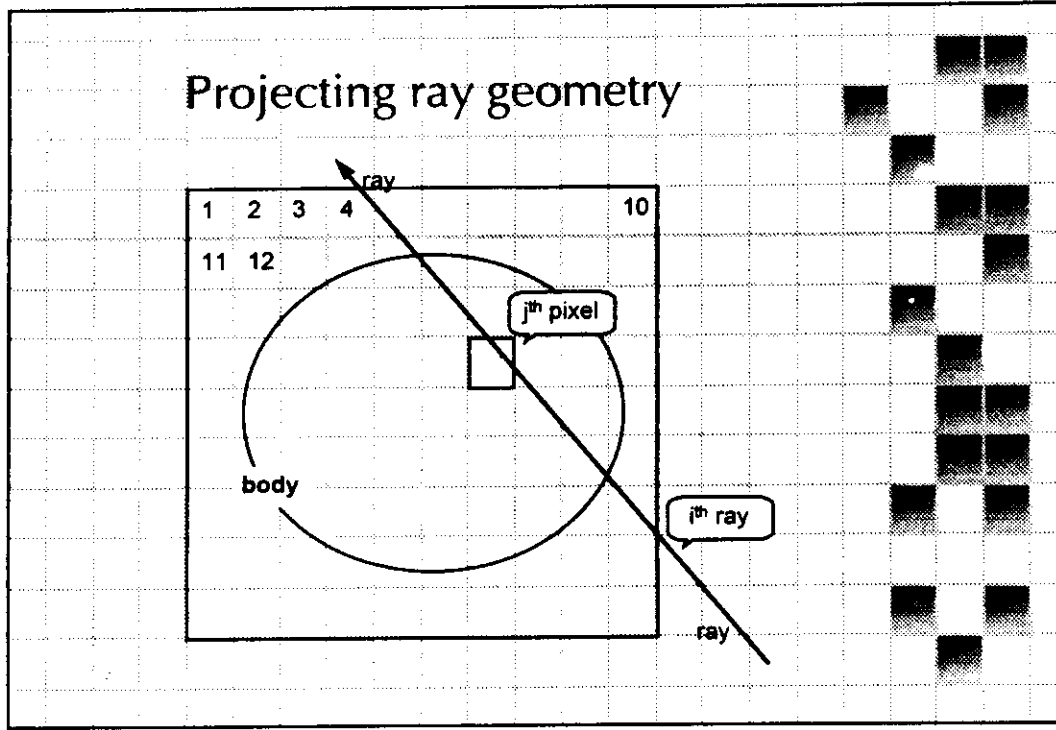
The [29] is simply the back-projection of all convolved projections.

The method so described is the well-known filtered back-projection (as the convolution is nothing but a filter) or convolution back-projection method.

The errors arising from the reconstruction methods are mainly due to technological limitations. These come from:

- a) insufficient sampling of the projection
- b) errors in estimation of  $\hat{p}$
- c) errors in the Fourier domain (interpolation, sampling).

As regards the comparison between the Fourier reconstruction and the convolution back-projection method, it has to be stressed that the latter has a far better performance. The Fourier reconstruction algorithm has its weakness in the inelegant 2-D interpolation required, producing images of bad quality. On the other hand, the Fourier algorithm has the potentiality of being performed with less computational effort in respect to the convolution back-projection one and this makes the Fourier algorithm worth of being investigated more in detail.



### FINITE SERIES-EXPANSION METHODS

In this family of reconstruction methods we are formulating a model which relates a finite set of known numbers with a finite set of unknown numbers. The resulting system of equations is then solved in a numerical way.

The line integral of the unknown attenuation function along the path of the ray can be expressed as in the figure above, where it is the sum of the products of the attenuation coefficient of each pixel multiplied by the length of the intersection of the ray  $i$  with the squared pixel  $j$  as:

$$\sum_{j=1}^n x_j \cdot a_{ij} \cong y_i \quad i = 1 \cdots m \quad [30]$$

In other words let us consider a set of basis functions in polar coordinates in plane:

$$\{b_j(r, \phi)\}_{j=1}^n \quad [31]$$

where

$$b_j(r, \phi) = \begin{cases} 1 & \text{if } (r, \phi) \in \text{pixel } j \\ 0 & \text{otherwise} \end{cases} \quad [32]$$

The digitalized image is then represented as:

$$\hat{f}(r, \phi) = \sum_{j=1}^n x_j \cdot b_j(r, \phi) \quad [33]$$

Using a set of continuous functionals which assign to any picture  $f(r, \phi)$  a real number  $\mathfrak{R}_i$ , we can say that  $\mathfrak{R}_i$  is the line integral of  $f(r, \phi)$  along the  $i^{\text{th}}$  ray.

Then:

$$y_i \cong \mathfrak{R}_{if} \cong \mathfrak{R}_{\hat{f}} = \sum_{j=1}^n x_j \cdot \mathfrak{R}_i \cdot b_j(r, \theta) = \sum_{j=1}^n x_j \cdot a_{ij} \quad [34]$$

so we obtain a set of equations:

$$\mathbf{y} = \mathbf{A} \cdot \mathbf{x} \quad [35]$$

Unfortunately the number of pixels  $n$  and the number of rays  $m$  are in the order of  $10^5$  and the direct matrix inversion is not generally feasible.

One of the best known reconstruction technique is the **Algebraic Reconstruction Technique or ART**.

This is an iterative method where the image matrix  $\mathbf{x}$  is initially assigned an arbitrary number. For each iteration the matrix  $\mathbf{x}$  is corrected (updated) by taking into account only a single ray and only the pixels intercepted by that ray. The discrepancy is then redistributed along the pixels intercepted.

In formulas:

$$\mathbf{x}^0 \in \mathfrak{R}^n \quad [36]$$

$$\mathbf{x}^{k+1} = \mathbf{x}^k + \frac{y_i - \langle a^i, \mathbf{x}^k \rangle}{\|a^i\|^2} \cdot a^i \quad [37]$$

where

$$\langle a^i, \mathbf{x}^k \rangle = \sum_{j=1}^n a_j^i \cdot x_j^k ; \|a^i\|^2 = \langle a^i, a^i \rangle ; a^i = (a_{ij})_{j=1}^n \quad [38]$$

The ART method, and those derived from that, are very useful in image reconstruction as they are feasible for various projective geometries.

They can also be used in high contrast images, when the reconstruction can make use only of a few directions of view, or when execution time is crucial.

## REFERENCES

The following references are quite complete reviews, giving a good perspective of reconstruction techniques and relative performances.

The papers may be very useful for better comprehension of the methods here presented in very general terms.

[1] Bates R.H.T., Garden K.L., Peters T.M., "Overview of computerized tomography with emphasis on future developments", Proc. IEEE, vol. 71, pp. 356-372, March 1983.

[2] Lewitt R.M., "Reconstruction algorithms: Transform methods", Proc. IEEE, vol. 71 pp. 390-408, March 1983.

[3] Censor Y., "Finite series-expansion reconstruction methods", Proc. IEEE, vol. 71, pp. 409-419, March 1983.